Nanostructures Formed by Calcium Substitution in Graphane

Erik Swenson

A senior thesis submitted to the faculty of
Brigham Young University
in partial fulfillment of the requirements for the degree of

Bachelor of Science

Bret Hess, Advisor

Department of Physics and Astronomy

Brigham Young University

April 2016

ABSTRACT

Nanostructures Formed by Calcium Substitution in Graphane

Erik Swenson
Department of Physics and Astronomy, BYU
Bachelor of Science

Because of its status as an emerging energy carrier, methods of hydrogen storage are in high demand. Using computational methods, we explore a very large space of graphene structures with different adsorption configurations of hydrogen and calcium as possible mechanisms for hydrogen storage. We expand our search space further than the traditional search space by a factor of almost 20 using cluster expansion to enumerate structures in a variety of computational cell shapes and sizes. This allows for periodicities not studied previously. We also introduce vacancies in the adsorption configurations and study their effects. We conclude that the cell size and shape is an important parameter in the search for stable structures. We also find that vacancies allow for structures with more than 40% calcium concentration without exhibiting signs of calcium stacking. We present four stable structures that show promise for hydrogen storage applications.

ACKNOWLEDGMENTS

Contents

List of Figures

Chapter 1

Introduction

1.1   Motivation

In the search for lightweight, space-efficient methods of energy storage, molecular hydrogen has emerged as a promising energy carrier. New clean fuel technologies (*e.g.* hydrogen fuel cells) take hydrogen molecules and convert the energy harnessed therein into electricity. Fuel technologies that utilize hydrogen energy are far less pollutant than standard hydrocarbon fuel sources such as gasoline or propane. Both production and consumption of hydrocarbon fuels can pose a risk to the people or the environment in densely populated cities or highly industrialized areas where these activities are prominent. Clean fuel technologies, on the other hand, pose much less of a risk when consumed.

We still need an external fuel source to *produce* the fuel technology itself, though. A hydrogen fuel cell, for example, needs a source of hydrogen. This means we need to obtain and isolate hydrogen molecules as well as produce some sort of structure that will store them, both of which require an outside energy source.

Finding an efficient and practical way to store hydrogen in large enough amounts is an in-

triguing problem. Hydrogen molecules are not naturally found in close proximity to one another. Containing hydrogen can be a difficult task as it is explosive and often requires high pressures and low temperatures. Alternatively, we can use a structure that is stable and holds hydrogen molecules in a tightly packed space, yet simple enough to manufacture in bulk amounts and safe enough for use in production. This paper is focused on searching for structures that meet these criteria.

1.2 Graphene and Hydrogen Storage

Graphene, an essentially two-dimensional hexagonal lattice of carbon atoms, was synthesized in 2004.[1] Graphene itself is incredibly strong, very thin, and an extremely good conductor of heat and electricty.[2] The high density of potentially bond-forming atoms and the two-dimensional nature of the material make graphene a natural starting point for hydrogen storage applications.[3] In fact, graphene has already proven to bond with atomic hydrogen in the form of a derivative structure called *graphane*.[4,5] This structure forms when a hydrogen atom bonds, or adsorbs, to each of the carbon atoms in the lattice. Throughout this paper, we will refer to any of these adsorption atoms bonded directly to the carbon monolayer as "adatoms".

In the graphane structure, the hydrogen atoms bond with both sides of the graphene sheet in an alternating top-bottom fashion (see Figure 1.1). A slight "buckling" is introduced to the lattice as a result of this bonding. The buckling is an important effect because it increases the tendency of the carbon atoms to bind other atoms.

However, graphane by itself is not very useful for hydrogen storage even though it has a hydrogen atom for every carbon atom in the lattice. Graphane is a very stable structure which makes extracting the hydrogen atoms an energy consuming task. To break the strong, covalent bonds (~ 2.5 $eV/atom$) that have formed between the carbon and hydrogen atoms, we would have to heat the structure—again drawing from another energy source—to the point that the energy lost
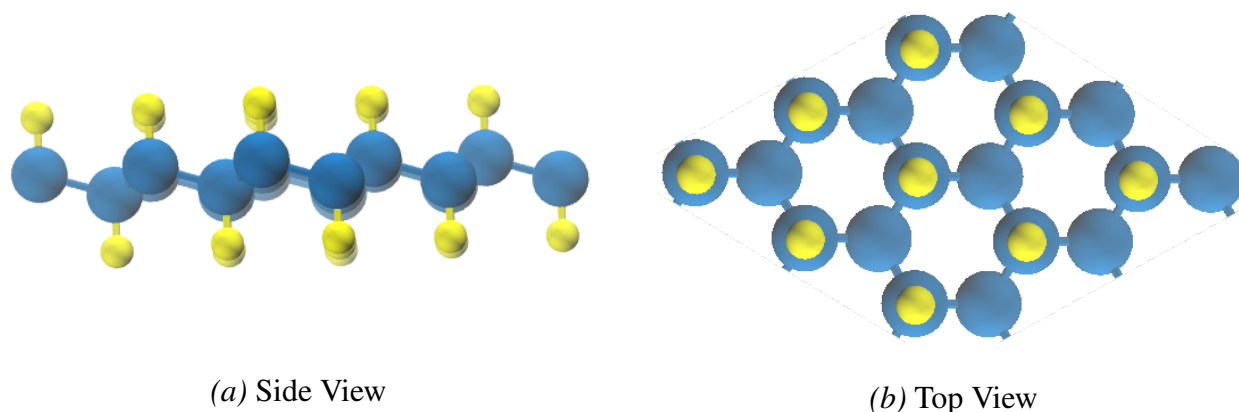
(a) Side View   *(b)* Top View

Figure 1.1 A visual depiction of the graphane structure. Note the alternating above-below scheme and lattice buckling apparent in *(a)*.

balances the energy gained. Even with that fact aside, atomic hydrogen (H) is much less useful as a fuel source than molecular hydrogen (H_2). We need a structure that binds pre-formed hydrogen molecules and, because of their stability, pure graphene and graphane do not.

We can remedy this problem by making a small modification to the graphane structure. By replacing some of the hydrogen adatoms with metal atoms, we can create a structure that might bind a reasonable amount of molecular hydrogen. The buckling induced in the graphene monolayer by the hydrogen atoms aids in the binding of these metals.

Computational work has already been performed examining calcium and lithium as the adatoms with promising results. Hussain *et al.* have explored both of these metals and report a hydrogen storage capacity of 6 wt. % for calcium[6] and 12 wt. % for lithium,[7–10] both with reasonable adsorption energies.

1.3   Our Project

In this paper, we explore computationally the possibility of using a graphene monolayer with calcium and hydrogen adatoms as a possible solution to the hydrogen storage problem. Our work goes beyond the previous work of Hussain *et al.*[6] in two ways.

Firstly, we allow for "vacancies"—carbon sites with no corresponding atom in the adsorbent monolayer. With vacancies in the structure, the calcium adatoms may have the ability to interact with more of the carbon atoms, producing higher binding energies between the carbon layer and the adatom layer. Larger spacing between the adatoms might also reduce the tendency of the calcium atoms to "stack", or build up in layers, allowing for higher concentrations of calcium in the structure and hopefully, by extension, increasing the structure's capacity for hydrogen storage.

Secondly, we examine structures from a multitude of computational unit cell sizes and shapes. This adds a significant degree of complexity to structure enumeration, but other members of our group have developed methods to speed up the computation.[11] Traditionally, only one diamond-shaped unit cell has been studied which greatly limits the possible atomic configurations that can be acheived. We use the UNiversal CLuster Expansion (UNCLE) code[12] to enumerate many different cell shapes that contain up to the same number of atoms as the traditional unit cell (see Figure 1.2). By using this type of structure enumeration, we hope to discover new structures with promising energetics.

We begin by briefly summarizing some key concepts and providing definitions for important terms. We will outline the computational algorithms used for structure enumeration, selection, and prioritization. We conclude with a presentation of the results we obtained. We compare structures with no vacancies against structures with vacancies and analyze what we find by searching a variety of cell shapes and sizes.

(a) Volume 7 (1×7) *(b)* Volume 9 (3×3)
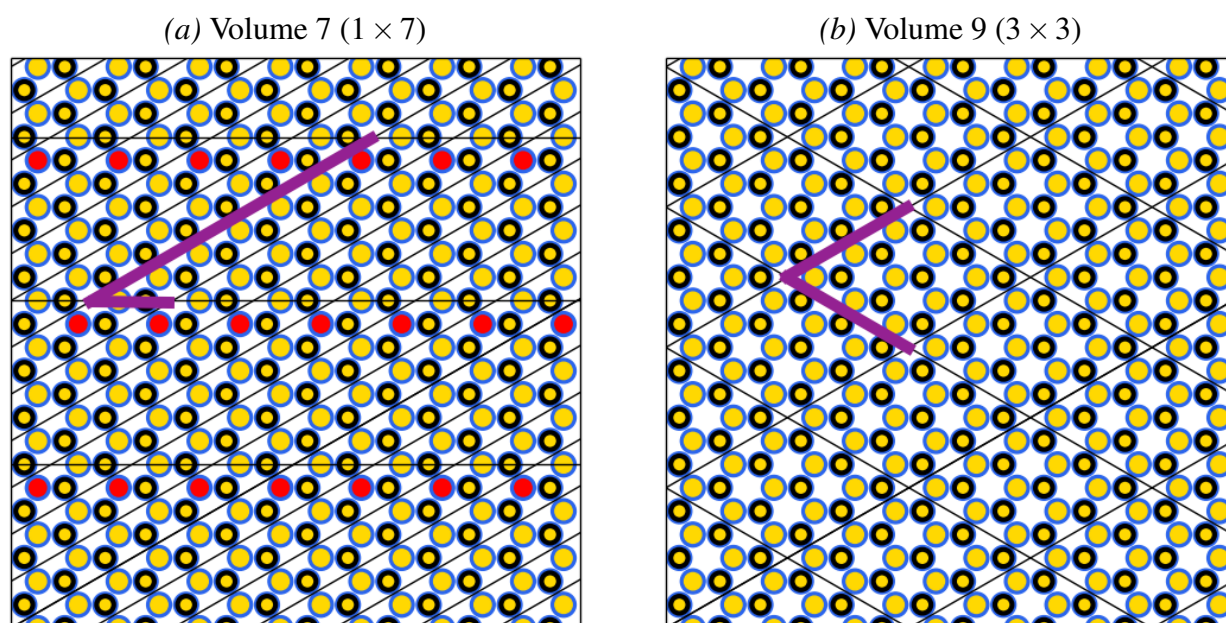
Figure 1.2 Two different examples of computational unit cells used in structure enumeration. These diagrams are two-dimensional representations of the structures we create. The blue circles represent carbon atoms in the graphene lattice. Yellow and red circles represent hydrogen and calcium adatoms respectively. A thick, black border around an adatom signifies that the atom is below the plane. The cells are defined by the lattice vectors highlighted in purple. The lattice vectors in *(b)* define the traditional unit cell, while the lattice vectors in *(a)* define a different periodicity. Note that the structure in *(b)* is a two-dimensional representation of the same structure pictured in Figure 1.1.

Chapter 2

Methods

2.1 Methods Common to Other Groups

2.1.1 Density Functional Theory

We ran energy calculations using the Vienna Ab-Initio Simulations Package (VASP)[13–16] code which performs calculations based on Density Functional Theory (DFT). DFT, as the name suggests, uses functionals of electron density to model atoms and their interactions. In the simplest of terms, a *functional* is a function of another function. In the case of modeling molecular structure energetics, the energy functional is of greatest interest. It takes in the electron density function over the entire cell and returns a scalar energy value. To find energetically favorable structures, then, the goal is to minimize the energy functional for each structure.

A drawback to DFT is that it is somewhat inaccurate in the calculation of weak van der Waals forces which play a large role in the carbon-hydrogen-metal systems being studied. At the heart of this problem is the fact that VASP makes use of two notable approximations to increase computational speed. In the Local Density Approximation (LDA), the energy functional only depends on the density at the point where the functional is being evaluated. A slightly modified approach

6

called the Generalized Gradient Approximation (GGA) is similar except that it also takes into account the gradient of the density at the point being evaluated. Both of these approximations have been shown to inaccurately represent the van der Waals interactions, with LDA overestimating and GGA underestimating.[6] That being said, for simulations with more than just a few atoms, these methods are industry standards and the best that we can do.

2.1.2 Cluster Expansion

Cluster Expansion (CE) provides a mathematical model from which we can predict the energies of a comprehensive space of structures based on the calculated energies of a few structures. CE gets its name from the "clusters", or combinations of occupied sites, that are summed together to represent a structure. Each cluster has an associated weight term which represents energy in this case. Clusters and their weights model the interaction between the atoms that make up the cluster. Clusters can be defined by a single atom (a 1-body cluster) or include any number of atoms in the lattice (an n-body cluster). As we include more clusters, the accuracy of the model increases until, in the limit of including all possible clusters, it approaches the actual energy of the structure. However, we can obtain excellent results even with a significant truncation. UNCLE truncates the expansion after 6-body clusters.

The cluster expansion model is defined by the following equation:

$$E_\sigma = \sum_c \Pi_{\sigma c} J_c \tag{2.1}$$

where σ represents a particular structure and c represents a particular cluster. The E_σ term represents the known (calculated) energy of the structure σ. The Π matrix is a matrix of correlation values between structures and clusters. The rows in the matrix represent structures and the columns represent clusters. Finally, the J_c term is an energy "weight" for a given cluster. For visualization's

sake, it may be easier to understand in matrix form.

$$
\begin{bmatrix} E_1 \\ E_2 \\ \vdots \\ E_n \end{bmatrix} = \begin{bmatrix} \Pi_{11} & \Pi_{12} & \cdots & \Pi_{1m} \\ \Pi_{21} & \Pi_{22} & \cdots & \Pi_{2m} \\ \vdots & \vdots & \ddots & \vdots \\ \Pi_{n1} & \Pi_{n2} & \cdots & \Pi_{nm} \end{bmatrix} \begin{bmatrix} J_1 \\ J_2 \\ \vdots \\ J_m \end{bmatrix}
\tag{2.2}
$$

In other words, the energy of a given structure is simply the sum of the properly weighted terms in the row of the Π matrix that represents the structure. If the Π matrix were square, we could simply invert the matrix and multiply to find the weights. However, the number of clusters and the number of structures do not have to be (and rarely are) equivalent. This generally results in a an underdetermined system for our purposes and more complex linear algebra techniques are required to solve it. Fortunately, Nelson *et al.* have developed Bayesian Compressed Sensing methods to solve this system efficiently.[17]

Once the weights are found, the multiplication on the right side of Eq. 2.1 predicts the energy for any structure in the space.

2.2 Enumeration of Structures

We use the UNCLE code to perform enumeration, or labeling, of all possible distinct structures in a given space. UNCLE performs a solely mathematical enumeration based on the shape of the lattice and the adatom options at each lattice site. This type of enumeration will inevitably produce structures that could not possibly exist in nature due to the size of the adatoms. For example, because the calcium-calcium bond length is large ($\sim$3.5 Å) and carbon-carbon bond lengths in the graphene lattice are smaller ($\sim$1.42 Å), we cannot physically place two calcium atoms adjacent to one another. Pairs of atoms that cannot be placed next to each other are termed *forbidden pairs*. We do not want to waste time in the search running "forbidden" structures through VASP calculations
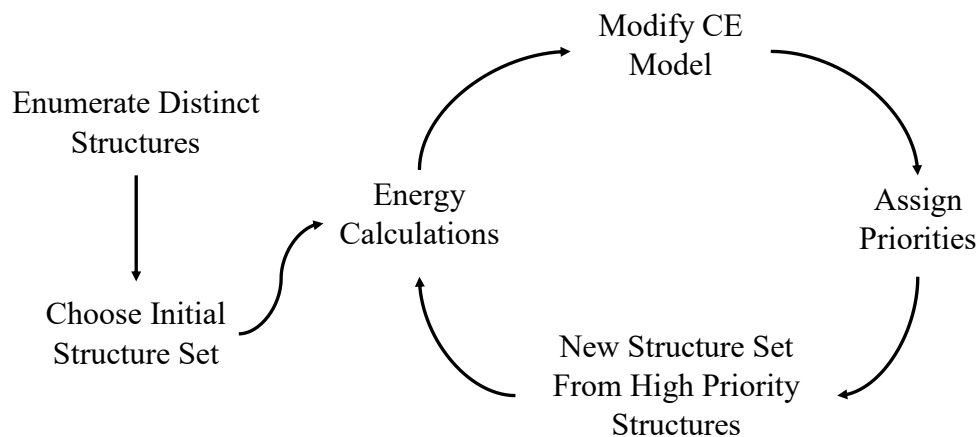
Figure 2.1 A high level map of the iteration process. We start with a "randomly" selected set of structures. We run the structures through energy calculations and use that data to create a predictive model for all possible structures. We then assign each structure a priority and choose a set of highest priority to run back through the loop. As more and more structures are calculated, the cluster expansion model becomes more and more accurate.

so, to this end, other members of our group have added functionality to exclude them from the enumeration.[11] Finally, from sets of structures that are rotationally or translationally equivalent (like 10 and 01) we only keep one.

2.3   Search for Favorable Structures

The main portion of my work in the group dealt with creating, coding, and automating the iterative process of searching the space of possible structures. The basic algorithm can be seen in Figure 2.1. It starts by selecting a set of what are called independently and identically distributed (IID) structures to use as initial input to the iteration loop. IID is a pseudo-random selection and means that the initial set will include structures that are as different as possible from one another.

Our new code takes the IID structure set and extracts the important information into a format that VASP can work with. VASP iteratively makes slight adjustments to the positions of the ions

and the electrons in order to minimize the energy of the structure in a process called *relaxation*.

Once VASP has found the energy-minimized configuration for each structure, we create a CE model based on the results from this initial structure set. The model predicts the energy of all the structures in the space. Initially, this model is not very accurate, but as we add more structures to the model each iteration, the accuracy increases substantially. We prioritize the structures according to a decaying exponential scale. Energetically favorable (low energy) structures at each concentration are given high priority while high energy structures are given a much lower priority.

We then select a new set of the highest priority structures from the pool of structures that have not been run through VASP calculations and the loop begins again. It should be noted that, because we choose new structures at the end of each iteration based on their priority, the energy-predictive model we refine may not be very accurate for higher energy structures. This is not an issue since high energy structures are of no practical interest to us anyway.

Chapter 3

Results and Conclusions

3.1 Energy Metrics

When analyzing the results of our energy calculations, the most useful metric we use to summarize a structure's energy is formation energy. Formation energy (FE) is defined as the average energy per adatom required to pull the adatoms out of reference structures and bind them to the graphene layer. For hydrogen, we use a hydrogen molecule as the reference structure and for calcium, the reference structure is a hexagonal monolayer of calcium atoms bound together. Mathematically,

$$\text{FE}_{struct} = \frac{\text{E}_{struct} - \left(\text{E}_{graphene} + \sum_i \text{n}_i \text{E}_i^{ref} \right)}{\sum_i \text{n}_i} \tag{3.1}$$

where E_{struct} is the energy value of that structure directly from the calculations, $\text{E}_{graphene}$ is the calculated reference energy of graphene, and the summation term gives the number of each type of adatom multiplied by its corresponding reference energy. The denominator simply tells us to divide by the number of adatoms.

Another important metric used in our analysis is planar binding energy (PBE) which, in the most simple terms, tells us how much energy is required per adatom to separate the adatom layers

from the carbon monolayer far enough that the interaction between the layers is negligible. In structures with positive or weakly negative PBE, it is likely that the adatoms will peel off the graphene as a separate group. Mathematically,

$$\text{PBE}_{struct} = \frac{\text{E}_{struct} - \left(\text{E}_{graphene} + \text{E}_{adatoms}\right)}{\sum_i n_i} \tag{3.2}$$

where E_{struct} and $\text{E}_{graphene}$ carry the same meaning as in FE and $\text{E}_{adatoms}$ represents the total energy of the adatom layers with the carbon atoms removed. Again, the summation term in the denominator tells us to divide by the number of adatoms.

Planar binding energy should not be confused with the standard binding energy (BE) of individual calcium atoms to the carbon-hydrogen structure. BE tells us how much energy it would take to pull the calcium atoms far enough away that they have no interaction with the rest of the structure. We will use BE as a comparison metric to other structures in the literature.

Our goal is to find structures that exhibit a strong FE as well as a strong PBE. To this end, we have defined a fourth, non-physical quantity called sorting energy (SE) which is defined as

$$\text{SE}_{struct} = max\left(\text{FE}_{struct}, \text{PBE}_{struct}\right) \quad . \tag{3.3}$$

When we sort the structures according to their SE, we can easily find those that have strong FE as well as PBE.

Figure 3.1 shows a plot of PBE vs. FE for binary double-sided structures. We can see that the region of interest representing structures that simultaneously boast low FE and PBE is basically empty. There are two tails of structures that skirt this region. The tail extending into the low FE region is mostly made up of structures that exhibit calcium stacking (discussed in the next section) and the tail extending into the low PBE region is mostly made up of "graphane-like" structures that contain no calcium at all. Neither of these are desirable characteristics for hydrogen storage applications and, thus, our focus will be on the structures that make some compromise between the two.
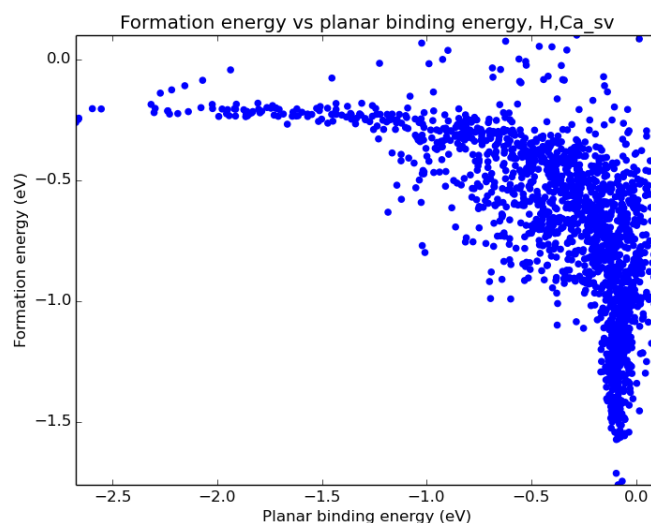
Figure 3.1 A plot of formation energy vs. planar binding energy for binary double-sided structures. Each blue dot represents a particular structure. The empty region in the lower left corner of the graph indicates that there is some sort of competition between the two types of energy.

3.2   Single-Sided Bonding

Figure 3.2 shows plots of formation energy vs. hydrogen concentration for binary single-sided structures. The red "tie lines" drawn in Figure 3.2 *(a)* define the *convex hull* of this set of structures. In thermal equilibrium, any structure that has formed will "settle" into sections that look like the structures on the convex hull. However, at this stage, we do not know anything about how long it will take to reach thermal equilibrium. A structure may not be the lowest energy structure at its concentration, but if the barriers to other lower energy states are high, it may take an impractically long time to reach the lowest energy state and is thus considered a *metastable* structure. With the information we currently have, we cannot rule out the possibility of any stable structure we find occurring in nature, even if it is not on the convex hull. We will focus on the structures with the strongest energies at each concentration, though, because they are the most *likely* to occur in nature.
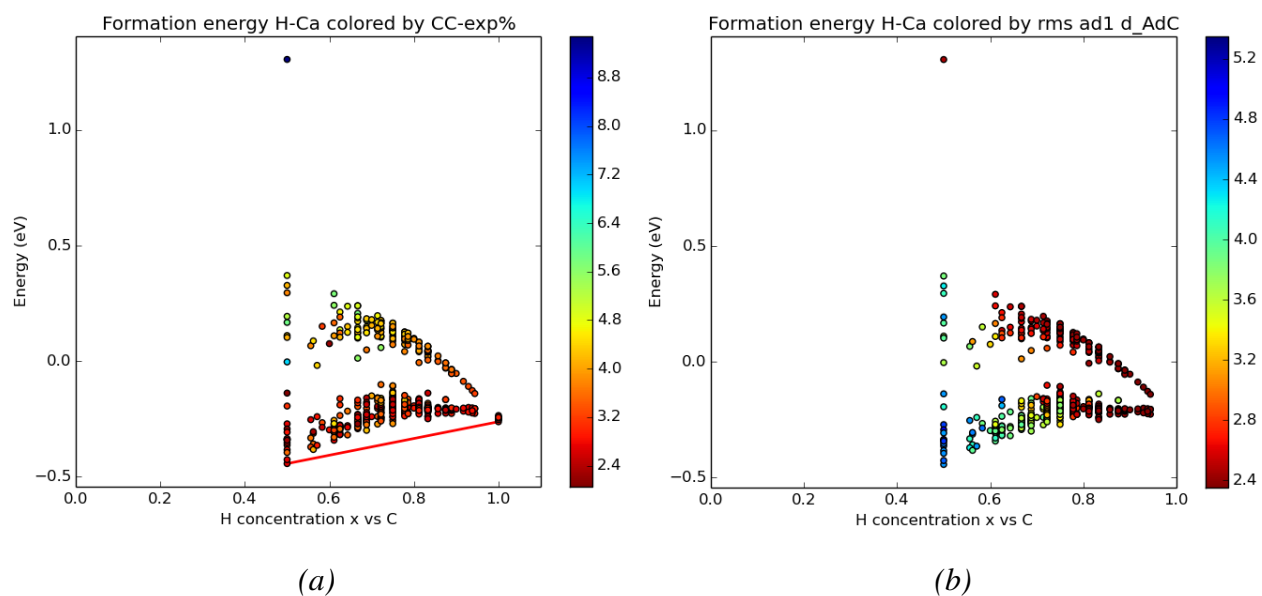
(a)   *(b)*

Figure 3.2 Plots of formation energy vs. hydrogen concentration in binary single-sided structures. The coloring of the dots in part *(a)* represents the expansion percentage of the carbon lattice as a result of adding the hydrogen and calcium. The red "tie lines" represent the convex hull: the naturally occurring structures in thermal equilibrium. The coloring of the dots in part *(b)* represents the average distance in angstroms of the calcium atoms from the plane of carbon atoms. "Stacked" structures have a much higher average calcium-carbon distance.

In the single-sided case, we find stable, desirable structures with up to 22% calcium concentration. At calcium concentrations greater than 22%, the lowest energy structures are less desirable due to "stacking" of calcium atoms perpendicular to the carbon monolayer rather than binding directly to the monolayer. Calcium stacking causes two main problems. Firstly, the stacked calcium atoms create strong bonds with each other, reducing the ability to bind H_2 to the structure. As the calcium atoms bond together, they build up and away from the plane of carbon atoms, making the structure much less space-efficient. The coloring of the dots in Figure 3.2 *(b)* indicates the average distance of the calcium atoms from the carbon monolayer. We can see that, above 22% calcium concentration, the average distance from the plane begins to increase due to calcium stacking. Secondly, the buildup of calcium layers adds extra weight to the structure. We want to create structures that are both space-efficient and lightweight and, therefore, we will discard any stacked structures from our analysis. An visual example of the stacking problem is shown in Figure 3.3.

The lowest energy binary single-sided structure at 22% calcium concentration is pictured in Figure 3.4 with FE $= -0.23$ *eV* and PBE $= -1.19$ *eV*. Since these energies are much stronger than thermal fluctuations (~ 30 *meV*), it is a stable structure. There are, of course, other structures at different concentrations with stronger energies, but we want to find those with the highest calcium concentrations and without calcium stacking. This structure fits both of those criteria.
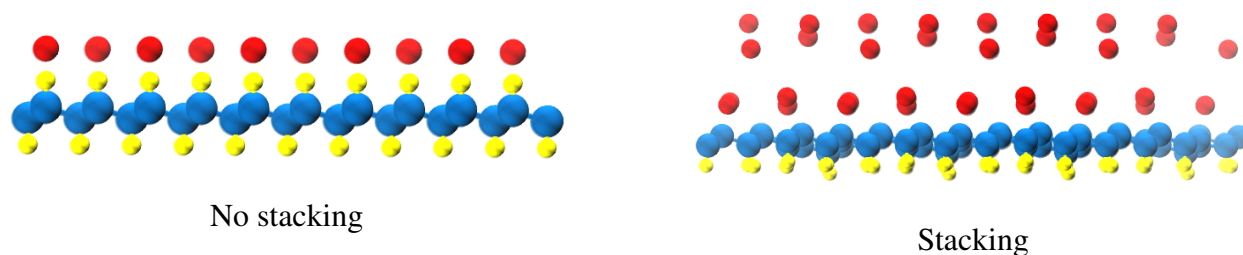

No stacking

Stacking

Figure 3.3 An example of calcium stacking. Pictured on the left is the side view of a structure where calcium atoms (red) and hydrogen atoms (yellow) are bound directly to the carbon monolayer (blue). On the right is the side view of a structure that exhibits calcium stacking. Calcium atoms bond with each other rather than the carbon monolayer and build up perpendicular to the plane, wasting valuable space in the structure.
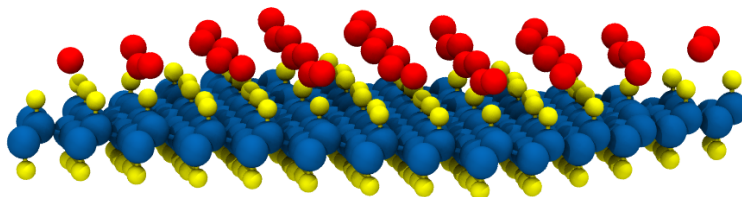
Figure 3.4 A rendering of the most stable binary single-sided structure at 22% calcium concentration without calcium stacking.

3.2.1   Estimating Error in the Energy Calculations

If we examine the formation energies closely, we can come up with an estimate of the error in the energy calculations. A pure graphane structure (100% hydrogen concentration) can be represented with any shape or size of computational unit cell, however, in the energy calculations, we should see the same result for each graphane structure regardless of cell shape or size. Looking at the plot of formation energy for single-sided structures shown in Figure 3.5, it is easy to see that there is some slight variation in the graphane calculations. Therefore, we cannot expect the error on any of the energy calculations to be smaller than that spread. The spread in the graphane energy calculations is 30 *meV* for FE and 20 *meV* for PBE. These error estimates should be applied to all energy calculations presented in this paper.

3.3   Double-Sided Bonding

After analyzing the results from the single-sided search, it is reasonable to expect that structures with high calcium concentrations will likely exhibit stacking. Our hope, though, is specifically to find structures with high calcium concentrations in order to bind higher concentrations of H_2 molecules later. Double-sided bonding results in a significant increase in the concentration of calcium atoms that can be achieved without stacking. Figure 3.6 shows the data from the binary double-sided search.
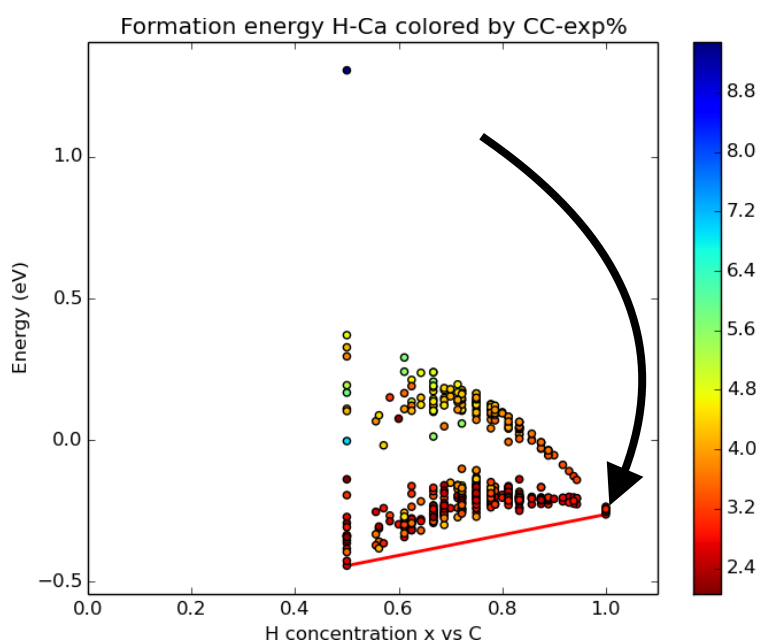
Figure 3.5 A plot of formation energy vs. hydrogen concentration with coloring representing the expansion percentage of the carbon lattice (also shown in Figure 3.2 *(a)*). The slight spread in the graphane energy calculations (indicated by the arrow) gives us an error estimate for all our energy calculations. The spread in formation energy is 30 *meV*.
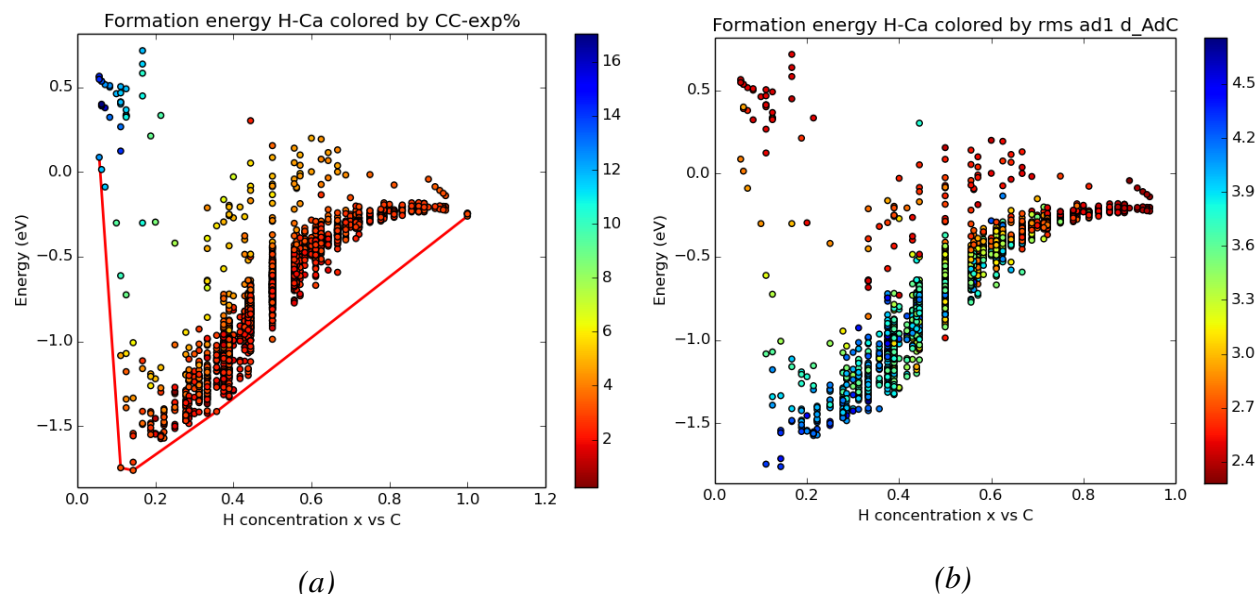
(a)   *(b)*

Figure 3.6 A plot of formation energy vs. hydrogen concentration for binary double-sided data. The coloring in these plots is similar to the coloring in Figure 3.2. The energies are similar to the single-sided case, but we can achieve a higher calcium concentration without stacking.
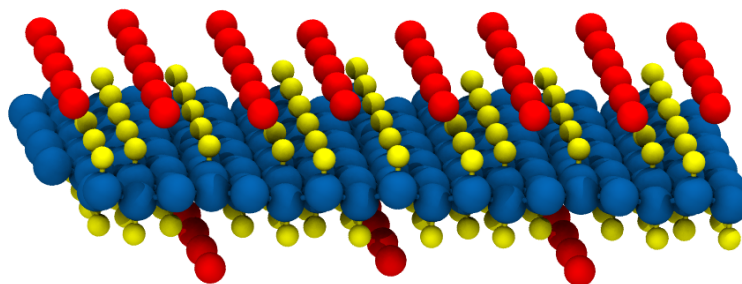

Figure 3.7 The binary double-sided structure with the highest concentration of calcium atoms (30%) that did not suffer from calcium stacking. Again, carbon atoms are blue, calcium atoms are red, and hydrogen atoms are yellow.

Focusing on the lowest energy structures at each calcium concentration in Figure 3.6 *(b)*, we see that stacking starts to occur above 30% calcium concentration. The most stable structure that we found at 30% calcium concentration is shown in Figure 3.7, with FE $= -330$ *meV* and PBE $= -690$ *meV*. Overall, though, the FE and PBE of binary double-sided structures are very similar, as evidenced by the plots in Figure 3.8.
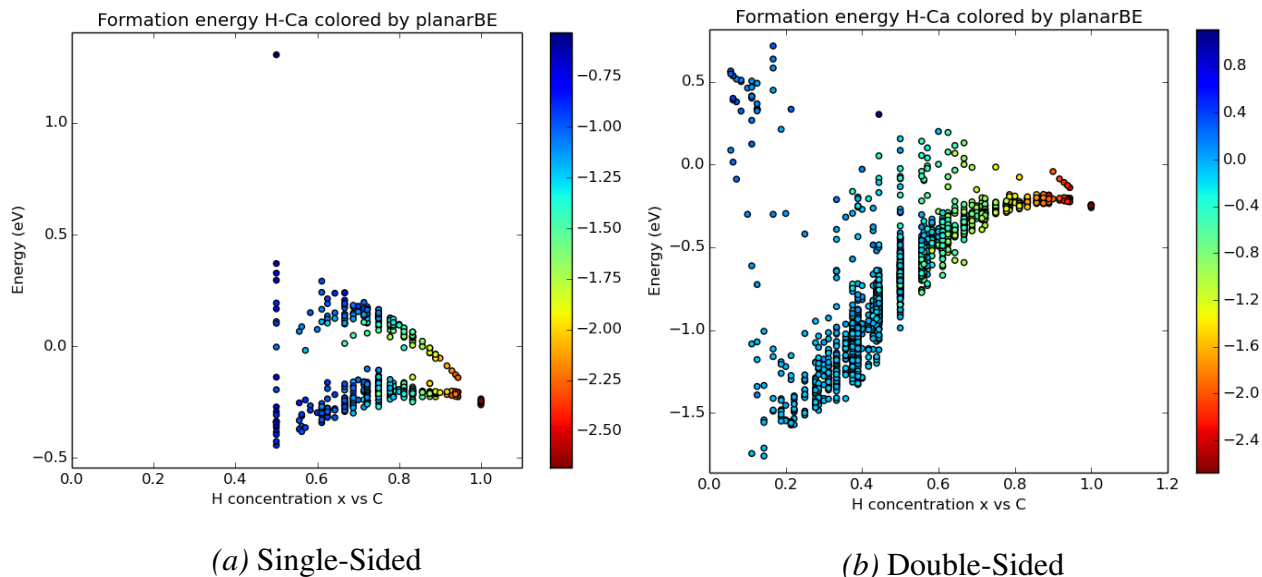
(a) Single-Sided

(b) Double-Sided

Figure 3.8 A side-by-side comparison of single-sided and double-sided data for binary structures. Notice the similar formation energies in the comparable region ($x > 0.8$) as well as the similar scale in planar binding energies.

Hussain, *et al.* also performed a binary double-sided search and presented a structure with 11.1% calcium concentration. They report a calcium BE of -2.4 *eV* per calcium atom.[6] The same structure in our search resulted in a calcium BE of -1.75 *eV* per calcium atom. The difference in calculations comes from two sources, both of which have been corroborated by the authors. First, they applied a van der Waals correction to their calculations, resulting in a stronger BE. Second, we calculate the BE of calcium atoms in a slightly different way. We compare the energy of the structure to the sum of the energy of the structure with the calcium atoms removed and the energy of the calcium atoms. In their calculations, they allow the structure with the calcium atoms removed to relax before summing with the energy of the calcium atoms. With this in mind, it is not unreasonable to see such a difference in calculations and we are confident that both calculations are valid.

As a testament to searching across multiple computational unit cells, our search returned four structures with stronger FE by up to 50 *meV* than the structure found by Hussain, *et al.* at the same
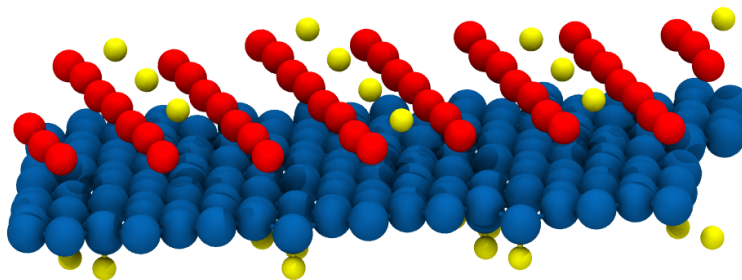
Figure 3.9 The most stable ternary single-sided structure with a calcium concentration of 25 %. Because of its stability and high calcium concentration, this structure shows great promise for hydrogen storage applications.

calcium concentration, all with non-traditional unit cells.

3.4 Effect of Vacancies

We have also studied ternary cases in which we allow three bonding options at each carbon site: a hydrogen atom, a calcium atom, or a vacancy. We find that allowing vacancies in our structure achieves still higher calcium concentrations without stacking effects.

We assume that the error in the energy calculations for ternary cases is similar to the error that was found in the binary cases and only report structures that are within that error ($\sim 30\ meV$) of the lowest calculated structure at each calcium concentration. We can then easily identify at what calcium concentration the calcium atoms begin to bond with each other and isolate from the graphene monolayer.

For the ternary single-sided case, we were able to find stable structures with calcium concentrations as high as 25% without stacking. This is a slight improvement ($\sim$3%) over the binary single-sided case. The most stable structure with a 25% calcium concentration (FE $= -2.15\ eV$ and PBE $= -0.74\ eV$) is pictured in Figure 3.9. Adding vacancies to the single-sided case, then, does not result in a large calcium concentration increase, but it does strengthen the FE by up to an order of magnitude.
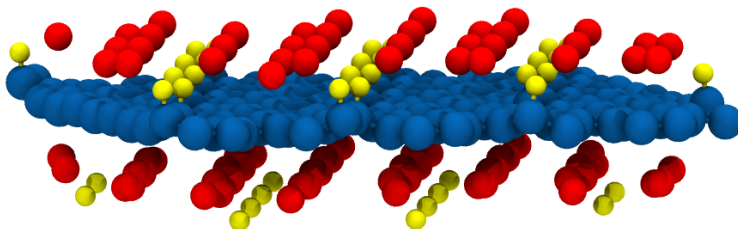
Figure 3.10 The most stable ternary double-sided structure with a calcium concentration of 44 %—a significant improvement over any other case we have studied.

For the double-sided case we found structures up to 44% calcium concentration without stacking—a considerable improvement over the binary double-sided case as well as the ternary single-sided case. The most stable double-sided structure with 44% calcium concentration (FE $= -1.981$ *eV* and PBE $= -0.199$ *eV*) is pictured in Figure 3.10. This structure also has a much stronger formation energy than the high concentration binary structure.

The comparisons made above show that vacancies play an important role in the formation of structures for hydrogen storage. We have shown that vacancies allow for higher concentrations of calcium atoms without giving way to stacking. It also appears that structures with vacancies have much stronger formation energy than their binary analogs. Both of these characteristics make structures with vacancies excellent candidates for hydrogen storage.

3.5   Variation of Unit Cells

As mentioned in Section 1.3, one of our objectives in this project was to expand our search by using a number of different computational unit cell shapes and sizes. It is clear that cell size and shape is an important parameter in the search for low energy structures.

For example, a full enumeration up through volume nine structures was performed for the binary double-sided case. Only 2,896 of 57,499 total distinct structures were of the traditional 3×3 unit cell type pictured in Figure 1.2 *(b)*. In fact, the overwhelming majority of the structures we

were interested in were not of that cell type. This result suggests that the periodicities encompassed by the volume nine, 3×3 unit cell may not be ideal periodicities for a C-H-Ca system. In any case, it is an important illustration of the fact that, in order to perform a complete search of the space, the size and shape of the unit cell must be a parameter in the search.

Bibliography

[1] K. S. Novoselov, A. K. Geim, S. V. Morozov, D. Jiang, Y. Zhang, S. V. Dubonos, I. V. Crig-orieva, and A. A. Firsov, "Electric Field Effect in Atomically Thin Carbon Films.," Science **306,** 666 – 669 (2004).

[2] C. Lee, X. Wei, J. W. Kysar, and J. Hone, "Measurement of the Elastic Properties and Intrinsic Strength of Monolayer Graphene," Science **321,** 385–388 (2008).

[3] M. Pumera, "Graphene-based nanomaterials for energy storage," Energy & Environmental Science **4,** 668–674 (2011).

[4] J. O. Sofo, A. S. Chaudhari, and G. D. Barber, "Graphane: A two-dimensional hydrocarbon," Physical Review B 75 (2007).

[5] D. C. Elias *et al.*, "Control of Graphene's Properties by Reversible Hydrogenation: Evidence for Graphane," Science **323,** 610–613 (2009).

[6] T. Hussain, B. Pathak, M. Ramzan, T. A. Maark, and R. Ahuja, "Calcium doped graphane as a hydrogen storage material," Applied Physics Letters 100 (2012).

[7] T. Hussain, A. De Sarkar, and R. Ahuja, "Strain induced lithium functionalized graphane as a high capacity hydrogen storage material," Applied Physics Letters 101 (2012).

[8] T. Hussain, T. Adit Maark, A. De Sarkar, and R. Ahuja, "Polylithiated (OLi2) functionalized graphane as a potential hydrogen storage material," Applied Physics Letters 101 (2012).

[9] T. Hussain, A. D. Sarkar, and R. Ahuja, "Functionalization of hydrogenated graphene by polylithiated species for efficient hydrogen storage," International Journal of Hydrogen Energy **39,** 2560 – 2566 (2014).

[10] T. Hussain, B. Pathak, T. A. Maark, C. M. Araujo, R. H. Scheicher, and R. Ahuja, "Ab initio study of lithium-doped graphane for hydrogen storage," EPL 96 (2011).

[11] J. Lawrence, Senior Thesis, Brigham Young University, 2016.

[12] D. Lerch, O. Wieckhorst, G. L. W. Hart, R. W. Forcade, and S. Müller, "UNCLE: a code for constructing cluster expansions for arbitrary lattices with minimal user-input," Modelling and Simulation in Materials Science and Engineering **17,** 055003 (2009).

[13] G. Kresse, "Ab initio molecular dynamics for liquid metals," Journal of Non-Crystalline Solids **192-193,** 222 – 229 (1995), structure of Non-Crystalline Materials 6.

[14] G. Kresse and J. Hafner, "*Ab initio* molecular-dynamics simulation of the liquid-metal–amorphous-semiconductor transition in germanium," Phys. Rev. B **49,** 14251–14269 (1994).

[15] G. Kresse and J. Furthmüller, "Efficiency of ab-initio total energy calculations for metals and semiconductors using a plane-wave basis set," Computational Materials Science **6,** 15 – 50 (1996).

[16] G. Kresse and J. Furthmüller, "Efficient iterative schemes for *ab initio* total-energy calculations using a plane-wave basis set," Phys. Rev. B **54,** 11169–11186 (1996).

[17] L. J. Nelson, V. Ozoliņš, C. S. Reese, F. Zhou, and G. L. W. Hart, "Cluster expansion made easy with Bayesian compressive sensing," Phys. Rev. B **88,** 155105 (2013).